

# A redetermination of the structure of the triple mutant (K53,56,120M) of phospholipase A<sub>2</sub> at 1.6 Å resolution using sulfur-SAS at 1.54 Å wavelength

K. Sekar,<sup>a,b,\*</sup> V. Rajakannan,<sup>c</sup>  
D. Velmurugan,<sup>c</sup> T. Yamane,<sup>d</sup>  
R. Thirumurugan,<sup>e</sup> M. Dauter<sup>f</sup>  
and Z. Dauter<sup>f</sup>

<sup>a</sup>Bioinformatics Centre, Indian Institute of Science, Bangalore 560 012, India,

<sup>b</sup>Supercomputer Education and Research Centre, Indian Institute of Science, Bangalore 560 012, India, <sup>c</sup>Department of Crystallography and Biophysics, University of Madras, Guindy Campus, Chennai 600 025, India, <sup>d</sup>Department of Biotechnology and Biomaterial Science, Graduate School of Engineering, Nagoya University, Furo-cho, Chikusa-ku, Nagoya 464-8603, Japan, <sup>e</sup>Department of Physiology and Biophysics, Ullmann Building, Room 315, Albert Einstein College of Medicine, 1300 Morris Park Avenue, Bronx, NY 10461, USA, and <sup>f</sup>SAIC-Frederick Inc., Basic Research Program, Brookhaven National Laboratory, Building 725A-X9, Upton, NY 11973, USA

Correspondence e-mail:  
sekar@physics.iisc.ernet.in

The crystal structure of the triple mutant K53,56,120M of bovine pancreatic phospholipase A<sub>2</sub> has been redetermined using sulfur single-wavelength anomalous scattering. The synchrotron data were collected at  $\lambda = 1.54 \text{ \AA}$  and the crystal diffracted to 1.6 Å resolution. The program *SOLVE* was used to locate the heavy atoms and to estimate the initial phases and the resulting map was then subjected to *RESOLVE*. The output of 455 non-H atoms, including 12 S atoms, one calcium ion and one chloride ion, were then subjected to *ARP/wARP* followed by *REFMAC*. With the improved phases, the automatic model building successfully built more than 85% of the 123 residues, excluding the N- and C-terminal residues. The final crystallographic *R* factor is 17.7% ( $R_{\text{free}} = 21.7\%$ ). The refined model consists of 954 non-H protein atoms, 165 water O atoms, three 2-methyl-2,4-pentanediol (MPD) molecules, one calcium ion and one chloride ion. The present work is yet another example that shows the utility of single-wavelength anomalous scattering data for solving a protein structure.

Received 3 May 2004

Accepted 12 July 2004

**PDB Reference:**

K53,56,120M PLA<sub>2</sub>, 1vkq,  
r1vkqsf.

## 1. Introduction

Macromolecular crystallography has now evolved to such an extent that structural genomics projects aiming at rapidly solving a large number of new structures in a short time are actively and successfully pursued in many laboratories. This is possible owing to the technological advances of crystallography, such as cryocrystallography, high-intensity synchrotron beamlines, production of selenomethionine protein variants by recombinant DNA techniques and significant methodological progress. One of the possibilities for speeding up X-ray data-collection and phasing procedures is to limit the number of data sets necessary to solve a structure using the MAD technique. If the anomalous diffraction signal of the scatterers (either introduced into the crystal or inherently present in the protein molecule) is measured accurately, it has been shown that only single-wavelength data (single-wavelength anomalous scattering; SAS) is sufficient to solve the structure. The success of this approach critically depends on the accuracy of measurement of the anomalous signal contained in the diffraction data. Hendrickson & Teeter (1981) originally showed that the anomalous signal of sulfur could be used to solve the structure of crambin. Later, Wang's simulations suggested that an anomalous signal as small as 0.6% of the total scattering might be sufficient for successful phasing (Wang, 1985). The anomalous scattering effect of sulfur was little exploited until the late 1990s. However, in recent years, mostly owing to advances in methodology, a revival of interest in this approach has taken place and many macromolecular structures have been solved using the

**Table 1**Peaks found by *SOLVE* and the corresponding atoms in the final model.

S No.	<i>SOLVE</i> peaks	Peak height <sup>†</sup>	Corresponding atoms
1	S1	52.26	Calcium ion
2	S2	27.53	Met8 SG
3	S3	20.61	Cys51 SG
4	S4	20.62	Cys105 SG
5	S5	22.43	Cys96 SG
6	S6	26.13	Cys44 SG
7	S7	17.22	Cys123 SG
8	S8	22.21	Cys84 SG
9	S9	17.79	Cys29 SG
10	S10	21.46	—
11	S11	20.81	—
12	S12	22.63	Cys98 SG
13	S13	16.27	—
14	S14	16.58	Chloride ion
15	S15	16.55	Cys91 SG
16	S16	17.36	Cys27 SG
17	S17	19.42	Cys45 SG

<sup>†</sup> The values are obtained from the anomalous difference Fourier map using the refined phases.

anomalous signal of S atoms (Bond *et al.*, 2001; Brown *et al.*, 2002; Dauter *et al.*, 1999; Debreczeni *et al.*, 2003; de Graaff *et al.*, 2001; Gordon *et al.*, 2001; Hendrickson & Teeter, 1981; Lemke *et al.*, 2002; Li *et al.*, 2002; Liu *et al.*, 2000; Micossi *et al.*, 2002; Olsen *et al.*, 2004; Ramagopal *et al.*, 2003; Wang, 1985; Yang & Pflugrath, 2001). Most sulfur-SAS applications have involved synchrotron radiation, sometimes at similar wavelengths to laboratory Cu *K* $\alpha$  sources (Dauter *et al.*, 1999), but usually at longer wavelengths where  $f''$  for sulfur is larger (Brown *et al.*, 2002; Gordon *et al.*, 2001; Liu *et al.*, 2000; Micossi *et al.*, 2002; Ramagopal *et al.*, 2003; Weiss *et al.*, 2001, 2004). In most of these studies, heavy atoms were located using either *SHELXD* (Schneider & Sheldrick, 2002) or *SnB* (Weeks & Miller, 1999). In addition, *SHARP* (de La Fortelle & Bricogne, 1997) and *wARP* (Perrakis *et al.*, 1999) are also used.

Rossmann (1961) was the first to propose the use of Bijvoet differences to locate anomalous scatterers. Direct methods have also been used to attempt to overcome the twofold ambiguity in the protein phases using the statistical relationship between phases and Bijvoet differences of selected reflections (Hauptman, 1997; Langs *et al.*, 1999; Liu *et al.*, 1999; Hao *et al.*, 2000). The data resolution limit seems to play a less important role, although it is obviously best to have accurate data at high resolution.

In principle, two AS data sets are necessary to estimate the protein phase uniquely. While collecting data at two wavelengths, it is always better to have one data set at a wavelength where  $f''$  is the largest for the anomalous scatterer (for the location of the anomalous scatterers) and the other data set at the highest possible resolution (Dauter, 2002). In this paper, we report the crystal structure of the triple mutant (K53,56,120M) of bovine pancreatic phospholipase A<sub>2</sub> redetermined using the S-SAS technique with synchrotron data (at 1.54 Å wavelength) collected to a resolution of 1.6 Å.

Phospholipase A<sub>2</sub> (PLA<sub>2</sub>) is a lipolytic enzyme that can be found both inside and outside cells. It is implicated in a variety of physiologically important cellular processes. PLA<sub>2</sub> specifi-

cally catalyses the hydrolysis of the fatty-acid ester bonds at the C2 position of 1,2-diacyl *sn*-3-phosphoglycerides. During the catalysis, the PLA<sub>2</sub> releases the fatty acid and the lysophospholipids. The product arachidonic acid is a precursor of the mediators of several inflammations and blood platelet aggregation. Biochemical studies revealed that lysine to methionine substitutions at positions 53, 56, 120 and 121 enhance the binding of the enzyme to the zwitterionic interface (Yu *et al.*, 2000).

As this paper is purely involved with the methodology of using sulfur anomalous scattering for solution of a macromolecular structure and since a detailed description of this triple mutant structure has already been published by our group (Sekar *et al.*, 2003), only a brief description is given of the structural aspects.

## 2. Diffraction data

The triple mutant (K53,56,120M) of bovine pancreatic PLA<sub>2</sub> was generated using site-directed mutagenesis (Noel *et al.*, 1991; Deng *et al.*, 1990; Sekar *et al.*, 2003). Crystals of the triple mutant were obtained using the hanging-drop vapour-diffusion method at room temperature (293 K) as described in Sekar *et al.* (2003). For data collection, a single crystal of dimensions 0.4 × 0.4 × 0.3 mm was transferred in a fibre loop and the diffraction data to 1.6 Å resolution (wavelength = 1.54 Å) were collected at a temperature of 100 K on the X9A synchrotron beamline at the National Synchrotron Light Source (Brookhaven National Laboratory, USA) using a MAR CCD detector system. The diffraction images were processed and intensities were merged using *HKL2000* (Otwinowski & Minor, 1997).

## 3. Phasing, model building and refinement

The average anomalous signal-to-noise ratio for the experimental data is 2.30. In order to locate the anomalous scatterers and to carry out the phasing, the automatic script *SOLVE/RESOLVE* (Terwilliger & Berendzen, 1999) was used. The present mutated protein contains 20 anomalous scatterers (18 S atoms, one calcium ion and one chloride ion). The output of *SOLVE* contained 17 peaks (Table 1): one calcium ion (topmost peak), one chloride ion and 12 S atoms. The remaining three are false-positive peaks and did not match with final positions of anomalous scatterers. The values of figure of merit ( $\langle m \rangle$ ) and the overall *Z* score at this stage are 0.31 and 25.31, respectively. The peak heights for all the anomalous scattering sites in the *SOLVE* map are greater than 11 $\sigma$ . The peaks from these phases were fed into *RESOLVE* for phase improvement and automatic model building. *RESOLVE* built the model, which had 67 amino-acid residues (455 atoms), in three segments. The map correlation coefficient between the SAS map and the final refined map was 0.49 and between the solvent-flattened map and the final refined map was 0.8574. The phases from *RESOLVE* were then input into *ARP/wARP* (Perrakis *et al.*, 1999). The starting *R* and *R*<sub>free</sub> values of the model were 50.6 and 53.2%, respectively. Ten cycles of model

building and ten cycles of *REFMAC* refinement (Murshudov *et al.*, 1999) were carried out for each cycle of model building, which led to a final model containing 114 amino-acid residues and 310 solvent atoms. The connectivity index was 0.97. The electron-density map phased using the 17 heavy atoms from *SOLVE* is shown in Fig. 1.

Manual model building was carried out for the N- and C-terminal residues and for the MPD molecules (present in the crystallization liquor). The water O atoms were located using the difference electron-density maps and minor model building was carried out for residues 3, 108 and 113 using the molecular-modelling program *FRODO* (Jones, 1985). Subsequently, the model was refined (ten cycles) using *REFMAC*. At this stage, the *R* and *R*<sub>free</sub> had converged to 17.7 and 21.7%, respectively. The pertinent refinement details along with the necessary statistics for the final protein model are given in Table 2.

## 4. Description of the structure

### 4.1. Quality of the model

The final model consists of 954 protein atoms, 165 water O atoms, three MPD molecules, one calcium ion and one chloride ion. Overall, the electron density is very clear for all the residues except the surface loop (residues 60–70). A Ramachandran ( $\varphi$ ,  $\psi$ ) map (Ramachandran & Sasisekharan, 1968) assessed using *PROCHECK* (Laskowski *et al.*, 1993) for the final model shows that 92.7% of all non-glycine residues are in the core region and the remaining residues are in additionally allowed regions. The average coordinate error estimated by the Cruikshank DPI method is 0.091 Å. A main-chain superposition of the present model with the structure of the trigonal (Sekar *et al.*, 1998; PDB code 1mkt) and ortho-

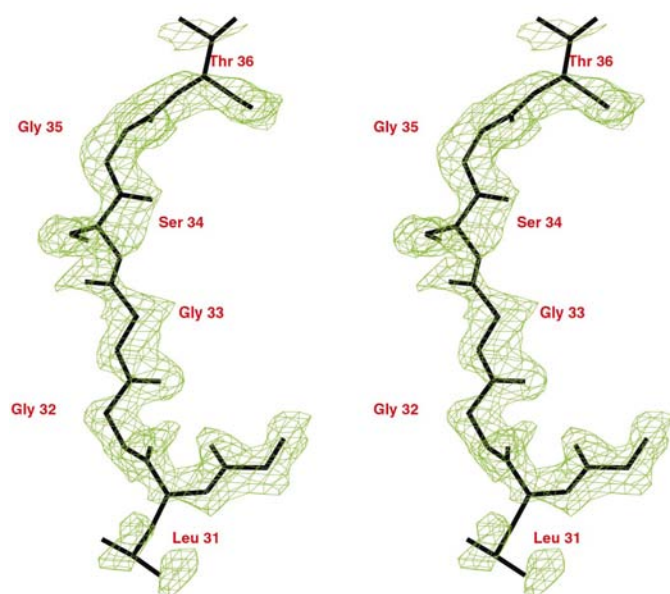


**Figure 1**  
A stereoview of a portion of the map from *SOLVE* (before density modification) along with the final model. The map is contoured at  $0.8\sigma$ .

**Table 2**  
Statistics of diffraction data and of refined model.

Intensity statistics	
Synchrotron source	BNL, NSLS
Beamline	X9A
Temperature (K)	100
Space group	<i>P</i> <sub>3</sub> 21
Wavelength (Å)	1.54
Unit-cell parameters (Å)	
<i>a</i> = <i>b</i>	46.05
<i>c</i>	101.58
Resolution range (Å)	20.0–1.6 (1.65–1.6)
Completeness (%)	100.0
<i>R</i> <sub>merge</sub>	0.059 (0.284)
<i>I</i> / $\sigma$ ( <i>I</i> )	50.1 (8.5)
Anomalous signal-to-noise ratio	2.30
Redundancy	12.1 (9.2)
Model details	
Protein atoms	954
Calcium ion	1
Chloride ion	1
MPD atoms	24
Water O atoms	165
Refinement	
<i>R</i> <sub>work</sub> (%)	17.7
<i>R</i> <sub>free</sub> (%)	21.7
Unique reflections	17048
Average <i>B</i> factor (Å <sup>2</sup> )	23.8
R.m.s deviations from ideal geometry	
Bond lengths (Å)	0.011
Bond angles (°)	1.536
Torsion angles (°)	5.620
Estimated overall coordinate error (Å)	0.091
Average temperature factors (Å <sup>2</sup> )	
Main-chain atoms	20.7
Side-chain atoms	23.4
Water molecules	37.0
Calcium ion	15.1
Chloride ion	17.7
MPD molecules	34.6

rhombic (Sekar & Sundaralingam, 1999; PDB code 1une) forms of the wild-type (WT) PLA<sub>2</sub> enzyme indicated that the overall tertiary fold is similar. The r.m.s. deviations are 1.11 and 0.23 Å, respectively, when the present structure is superimposed (backbone atoms only) with the monoclinic form of the triple mutant (K56,120,121M; Rajakannan *et al.*, 2002; PDB code 1gh4) and the trigonal form of the double mutant (K53,56M; Yu *et al.*, 2000; PDB code 1c74). In the present structure, the surface-loop region (residues 60–70) is disordered, as was the case in most recombinant bovine PLA<sub>2</sub> structures studied so far (Sekar *et al.*, 1997, 1998, 1999).

### 4.2. Chloride ion

A peak was located by *SOLVE* near the N-terminal region at  $11\sigma$  level in the *SOLVE* map. According to the crystallization conditions and the chemical environment around this peak, it was treated as a chloride ion. A recent atomic resolution structure of PLA<sub>2</sub> (Steiner *et al.*, 2001) showed the presence of a chloride ion at the same position. It has three ligands: the N atom (NZ) of the residue Lys12, the backbone N atom of Ile82 and a water molecule at distances 3.16, 3.19 and 3.07 Å, respectively (Fig. 2). It is interesting to note that this is the first report of chloride ion in the recombinant

bovine pancreatic PLA<sub>2</sub> structure and there is no literature evidence available regarding its biological implications.

#### 4.3. MPD molecules

In the present refined protein model three MPD molecules are found. One MPD is located in the active-site mouth and this molecule was observed in our previous studies (Sekar *et al.*, 2003; Rajakannan *et al.*, 2002). The remaining MPD molecules are located near the surface of the protein (Glu17/Lys108 and Ser15/Ser16); similar binding of MPD molecules was also observed in the recently reported WT structure (Steiner *et al.*, 2001).

#### 4.4. Water structure

The present protein model is hydrated by 165 water molecules; of these, 139 water molecules are in the first hydration shell, while 22 are in the second hydration shell. The remaining four water molecules do not have contacts and are treated as isolated water molecules. The first hydration shell water molecules are involved in 404 contacts (between 2.25 and 3.6 Å) with protein atoms; of these, 121 contacts are with the backbone polar atoms and 124 contacts with side-chain polar atoms. 65 water molecules are common (within 1.8 Å distance after superposition; Biswal *et al.*, 2000) to the present model and our previously reported 1.85 Å resolution structure (Sekar *et al.*, 2003), which contained 85 water molecules.

#### 4.5. Comparison with our earlier structure refined at 1.85 Å

17 048 reflections are used in the present refinement compared with 11 698 reflections in our earlier refinement (Sekar *et al.*, 2003). The r.m.s. deviations from ideal geometry of the present model (Table 2) are better than the values reported previously. A superposition of the backbone atoms of the two protein models gave an r.m.s. deviation of 0.22 Å. It is noteworthy that the surface-loop residues are disordered in both structures. The chloride ion in the present model was detected by *SOLVE* and the corresponding position in the previously reported structure was modelled as a water O atom.

### 5. Conclusions

The present paper emphasizes the applicability of the S-SAS technique to solving a macromolecular structure when data extends to 1.6 Å resolution. Although the absorption edge of sulfur is close to 5 Å, even at 1.54 Å wavelength the anomalous signal contributed by the S atoms was sufficient to reveal their locations using *SOLVE*. This work also adds substantial evidence that even with single-wavelength anomalous scattering data a macromolecular structure can be solved with the existing sophisticated programs.

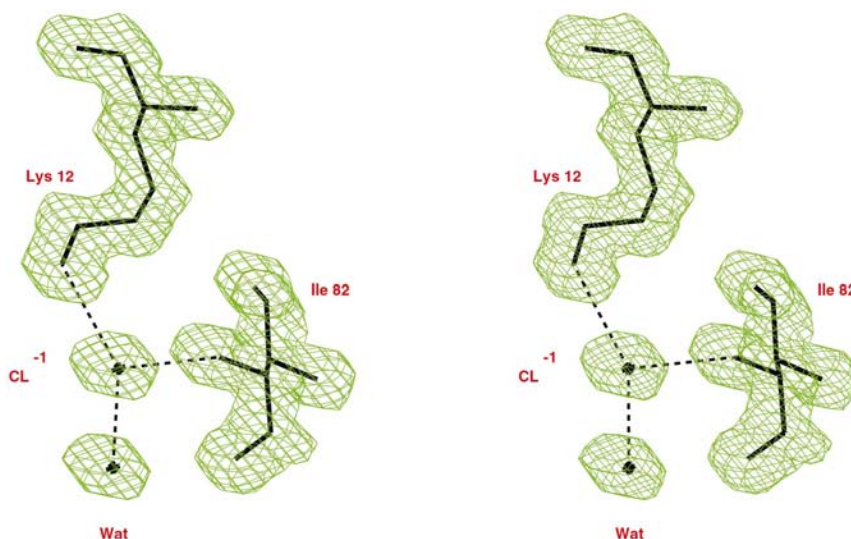


**Figure 2**

A stereoview of the omit electron-density map showing the chloride ion and its liganded atoms. Contours are shown at  $1.2\sigma$ .

The authors gratefully acknowledge the use of the Bioinformatics Centre, the interactive graphics-based molecular-modelling facility and the Supercomputer Education and Research Centre at the Indian Institute of Science, Bangalore. DV thanks the Department of Science and Technology, Government of India and the University Grants Commission, India for support and SAIC-Frederick Inc., Basic Research Program, BNL, USA for a visiting scientist fellowship. Part of this work was carried out at the Department of Biotechnology, School of Engineering, Nagoya University, Nagoya, Japan under the VBL visiting professorship scheme awarded to DV and KS. VR thanks the Council of Scientific and Industrial research for a Senior Research Fellowship.

### References

- Biswal, B. K., Sukumar, N. & Vijayan, M. (2000). *Acta Cryst.* **D56**, 1110–1119.
- Bond, C. S., Shaw, M. P., Alphey, M. S. & Hunter, W. N. (2001). *Acta Cryst.* **D57**, 755–758.
- Brown, J., Esnouf, R. M., Jones, M. A., Linnell, J., Harlos, K., Hassan, A. B. & Jones, E. Y. (2002). *EMBO J.* **21**, 1054–1062.
- Dauter, Z. (2002). *Acta Cryst.* **D58**, 1958–1967.
- Dauter, Z., Dauter, M., de La Fortelle, E., Bricogne, G. & Sheldrick, G. M. (1999). *J. Mol. Biol.* **289**, 83–92.
- Debreczeni, J. E., Bunkoczi, G., Girmann, B. & Sheldrick, G. M. (2003). *Acta Cryst.* **D59**, 393–395.
- Deng, T., Noel, J. P. & Tsai, M.-D. (1990). *Gene*, **93**, 229–234.
- Graaff, R. A. G. de, Hilge, M., van der Plaas, J. L. & Abrahams, J. P. (2001). *Acta Cryst.* **D57**, 1857–1862.
- Gordon, E. J., Leonard, G. A., McSweeney, S. & Zagalsky, P. F. (2001). *Acta Cryst.* **D57**, 1230–1237.
- Hao, Q., Gu, Y. X., Zheng, C. D. & Fan, H. F. (2000). *J. Appl. Cryst.* **33**, 980–981.
- Jones, T. A. (1985). *Methods Enzymol.* **115**, 157–171.
- Hauptman, H. A. (1997). *Curr. Opin. Struct. Biol.* **7**, 672–680.
- Hendrickson, W. A. & Teeter, M. M. (1981). *Nature (London)*, **290**, 107–113.

- La Fortelle, E. de & Bricogne, G. (1997). *Methods Enzymol.* **276**, 472–494.
- Langs, D. A., Blessing, R. H. & Guo, D. Y. (1999). *Acta Cryst.* **A55**, 755–760.
- Laskowski, R. A., MacArthur, M. W., Moss, D. S. & Thornton, J. M. (1993). *J. Appl. Cryst.* **26**, 283–291.
- Lemke, C. T., Smith, G. D. & Howell, P. L. (2002). *Acta Cryst.* **D58**, 2096–2101.
- Li, S., Finley, J., Liu, Z.-J., Qiu, S.-H., Chen, H., Luan, C.-H., Carson, M., Tsao, J., Johnson, D., Lin, G., Zhao, J., Thomas, W., Nagy, L. A., Sha, B., DeLucas, L. J., Wang, B.-C. & Luo, M. (2002). *J. Biol. Chem.* **277**, 48596–48601.
- Liu, Y. D., Harvey, I., Gu, Y. X., Zheng, C. D., He, Y., Fan, H., Hasnain, S. S. & Hao, Q. (1999). *Acta Cryst.* **D55**, 1620–1622.
- Liu, Z.-J., Vysotski, E. S., Chen, C.-J., Rose, J. P., Lee, J. & Wang, B.-C. (2000). *Protein Sci.* **9**, 2085–2093.
- Micossi, E., Hunter, W. N. & Leonard, G. A. (2002). *Acta Cryst.* **D58**, 21–28.
- Murshudov, G. N., Lebedev, A., Vagin, A. A., Wilson, K. S. & Dodson, E. J. (1999). *Acta Cryst.* **D55**, 247–255.
- Noel, J. P., Bingman, C. A., Deng, T., Dupureur, C. M., Hamilton, K. J., Jiang, R. T., Kwak, J. G., Sekharudu, C., Sundaralingam, M. & Tsai, M.-D. (1991). *Biochemistry*, **30**, 11801–11811.
- Olsen, J. G., Flensburg, C., Olsen, O., Bricogne, G. & Henriksen, A. (2004). *Acta Cryst.* **D60**, 250–255.
- Otwinowski, Z. & Minor, W. (1997). *Methods Enzymol.* **276**, 307–326.
- Perrakis, A., Morris, R. J. & Lamzin, V. S. (1999). *Nature Struct. Biol.* **6**, 458–463.
- Rajakannan, V., Yogavel, M., Poi, M. J., Jeya Prakash, A. A., Jeyakanthan, J., Velmurugan, D., Tsai, M.-D. & Sekar, K. (2002). *J. Mol. Biol.* **324**, 755–762.
- Ramachandran, G. N. & Sasisekharan, V. (1968). *Adv. Protein Chem.* **23**, 283–291.
- Ramagopal, U. A., Dauter, M. & Dauter, Z. (2003). *Acta Cryst.* **D59**, 1020–1029.
- Rossmann, M. G. (1961). *Acta Cryst.* **14**, 383–388.
- Schneider, T. R. & Sheldrick, G. M. (2002). *Acta Cryst.* **D58**, 1772–1779.
- Sekar, K., Biswas, R., Li, Y., Tsai, M.-D. & Sundaralingam, M. (1999). *Acta Cryst.* **D55**, 443–447.
- Sekar, K., Sekharudu, C., Tsai, M.-D. & Sundaralingam, M. (1998). *Acta Cryst.* **D54**, 342–346.
- Sekar, K. & Sundaralingam, M. (1999). *Acta Cryst.* **D55**, 46–50.
- Sekar, K., Vijayanthi Mala, S., Yogavel, M., Velmurugan, D., Poi, M. J., Vishwanath, B. S., Gowda, T. V., Jeyaprakash, A. A. & Tsai, M.-D. (2003). *J. Mol. Biol.* **333**, 367–376.
- Sekar, K., Yu, B.-Z., Rogers, J., Lutton, J., Liu, X., Chen, X., Tsai, M.-D., Jain, M. K. & Sundaralingam, M. (1997). *Biochemistry*, **36**, 3104–3114.
- Steiner, R. A., Rozeboom, H. J., de Vries, A., Kalk, K. H., Murshudov, G. N., Wilson, K. S. & Dijkstra, B. W. (2001). *Acta Cryst.* **D57**, 516–526.
- Terwilliger, T. C. & Berendzen, J. (1999). *Acta Cryst.* **D55**, 849–861.
- Wang, B.-C. (1985). *Methods Enzymol.* **115**, 90–112.
- Weeks, C. M. & Miller, R. (1999). *J. Appl. Cryst.* **32**, 120–124.
- Weiss, M. S., Mander, G., Hedderich, R., Diederichs, K., Ermler, U. & Warkentin, E. (2004). *Acta Cryst.* **D60**, 686–695.
- Weiss, M. S., Sicker, T., Djinic Carugo, K. & Hilgenfeld, R. (2001). *Acta Cryst.* **D57**, 689–695.
- Yang, C. & Pflugrath, J. W. (2001). *Acta Cryst.* **D57**, 1480–1490.
- Yu, B.-Z., Poi, M. J., Ramagopal, U. A., Jain, R., Ramakumar, S., Berg, O. G., Tsai, M.-D., Sekar, K. & Jain, M. K. (2000). *Biochemistry*, **39**, 12312–12323.